

Article

## A COMPARATIVE STUDY ON THE OBTAINING OF ALPHA- $\text{Fe}_2\text{O}_3$ NANOPARTICLES BY TWO DIFFERENT SYNTHESIS METHODS

*Oana Stefanescu<sup>1\*</sup>, Corneliu Davidescu<sup>1</sup>, Cornelia Muntean<sup>1</sup>*

<sup>1</sup>Politehnica University Timisoara, Applied Chemistry and Inorganic Compounds Engineering, 6 Vasile Parvan Blvd., 300223, Timisoara, Romania

### ABSTRACT

This paper deals with the synthesis of  $\alpha\text{-Fe}_2\text{O}_3$  nanoparticles by two different synthesis methods: precipitation and thermal decomposition of carboxylate complex. The effect of temperature on the characteristics of the obtained powders was investigated by thermal analysis, XRD, FTIR spectroscopy and SEM. This study compares the results obtained by the two methods mentioned above, in which the mechanism of  $\alpha\text{-Fe}_2\text{O}_3$  formation is different. The iron hydroxide precipitate obtained at 90°C was annealed at 300°C with formation of  $\alpha\text{-Fe}_2\text{O}_3$  nanoparticles. By thermal decomposition of the Fe(III) carboxylate combination at 300°C, the cubic  $\gamma\text{-Fe}_2\text{O}_3$  is obtained, which turns to hexagonal  $\alpha\text{-Fe}_2\text{O}_3$  nanoparticles, at 500°C.

**Keywords:** carboxylate combination, precipitation,  $\alpha\text{-Fe}_2\text{O}_3$ , nanoparticles

### 1. INTRODUCTION

The methods used for the synthesis of iron oxides are from the most different ones assuring specific performances to the resulted oxide. Each method presents advantages regarding some applications and disadvantages regarding other applications. Thus, it is explained that the usage of different synthesis methods result in oxides with different morphologies. The particularity of iron oxides synthesis methods is to obtain well crystallized, single phases. The materials research is focused on the obtaining of iron oxides nanoparticles due to the unique dependence of the properties on the nanoparticle size [1]. The

---

\* Correspondent author: Tel:+40737686813, E-mail: oanaelenastefanescu@yahoo.com

researchers concerns are oriented towards an efficient control on purity, homogeneity, porosity, grain size, grain size distribution, morphology and phase composition, all these factors being decisive for the characteristics of the final product. The choice of the most suitable synthesis method for the iron oxides and the identification of the optimal synthesis conditions ensure the premise for the maximization of its advantages [2]. Among iron oxides, hematite ( $\alpha\text{-Fe}_2\text{O}_3$ ) is widely studied due to its applications as pigment, sensor, electrode material and recently photocatalyst [3-6].  $\alpha\text{-Fe}_2\text{O}_3$  is the most stable iron oxide with high resistance to corrosion, low cost, biocompatibility, high efficiency, non-toxic characteristics [3, 7]. In the last years, the researchers have developed some unconventional methods and precursors for the obtaining of hematite with specific properties, such as: the hydrothermal method, precipitation, the sol-gel method, combustion [8-12]. These methods present a series of advantages: homogeneous distribution of the oxide at molecular scale, high reactivity, fine granulation, high specific surface and porosity, due to low formation temperatures, control on particles sizes.

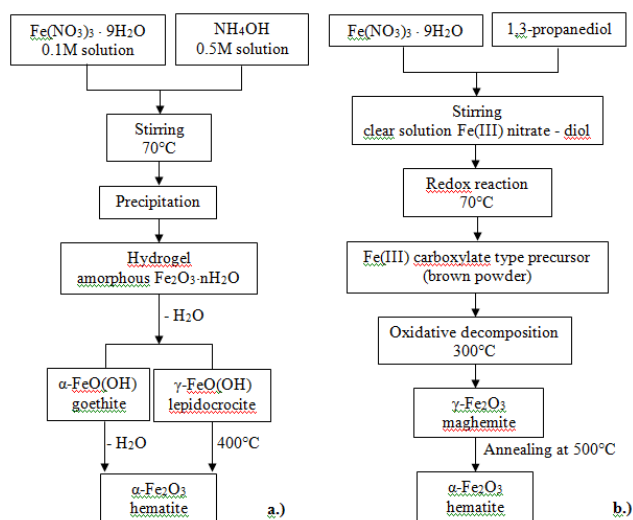
## 2. METHOD

The purpose of this paper is to illustrate and compare two synthesis methods, precipitation of Fe(III) hydroxide and thermal decomposition of Fe(III) carboxylate type precursors, for the obtaining of  $\alpha\text{-Fe}_2\text{O}_3$ . This approach will provide a better insight on the influence of the starting precursor on the formation and features of  $\alpha\text{-Fe}_2\text{O}_3$ .

### 2.1. Theoretical Method

The methods used show two different preparation procedures for  $\alpha\text{-Fe}_2\text{O}_3$ , as in Fig.1 (a,b).

**Figure 1:** General schemes for the preparation of  $\alpha\text{-Fe}_2\text{O}_3$  nanoparticles, by: a.) precipitation, b.) thermal decomposition of Fe(III) carboxylate type precursors



### *Precipitation*

Iron (III) nitrate nine-hydrate as iron source and ammonium hydroxide as precipitating agent were used, both of analytical purity and purchased from Merck. These reagents were used to prepare iron oxide particles. Iron (III) nitrate was dissolved in distilled water, with stirring, to give a 0.1M solution. 0.5 M ammonium hydroxide solution was added drop wise into the 0.1M iron nitrate solution under vigorous stirring. The volume ratio of the solutions was 1:1. The resulted product was a dark brown precipitate, which was filtered, washed three times with distilled water and dried at 90°C, 20h. The sample was further annealed at 200°C, 300°C and 500°C, 3h.

### *Thermal decomposition of Fe(III) carboxylate type precursors*

There was synthesized a precursor of Fe(III) carboxylate type starting from iron(III) nitrate nine-hydrate and 1,3-propandiol (1,3PG), both of analytical purity purchased from Merck. 0.0375 moles Fe(NO<sub>3</sub>)<sub>3</sub>·9H<sub>2</sub>O were solubilised in 0.0633 moles 1,3PG until a homogenous, viscous mixture was formed. The reagent quantities were calculated according to the reaction stoichiometry [13] with a diol excess of 50% for the obtaining of 3g Fe<sub>2</sub>O<sub>3</sub>. The resulted mixture was heated in an oven, when the redox reaction between the NO<sub>3</sub><sup>-</sup> and diol, took place at ~70°C, with formation of the Fe(III) carboxylate combination. The decomposition of the complex combination at 300°C led to  $\gamma$ -Fe<sub>2</sub>O<sub>3</sub> (maghemite) [14]. By direct annealing of the complex combination at 500°C,  $\alpha$ -Fe<sub>2</sub>O<sub>3</sub> (hematite) was obtained.

## **2.2. Experimental Method**

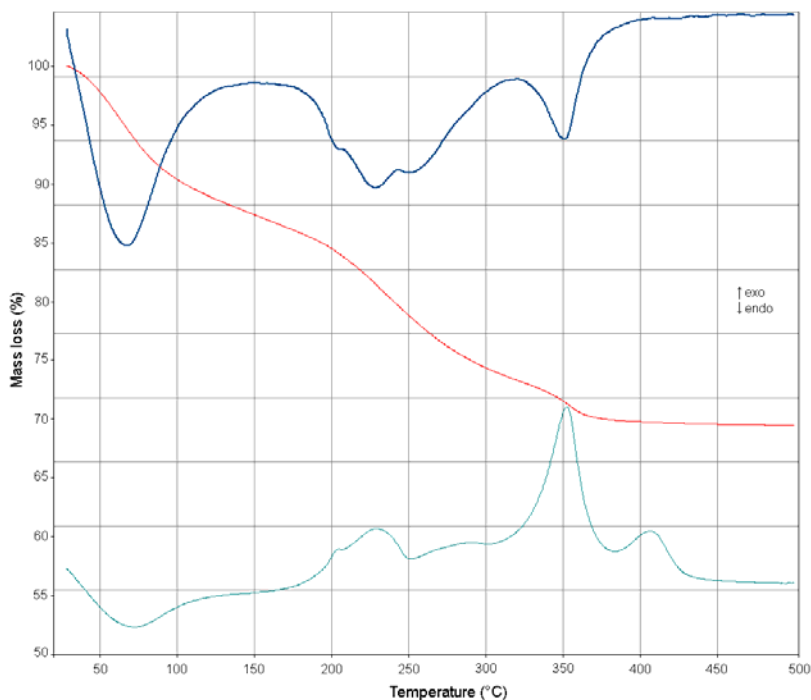
Thermal analysis studies were carried out using a 1500 D MOM Budapest derivatograph in air, in the temperature range 25 – 500°C, with a heating rate of 5°C/min, using a sample mass of ~ 100 mg and  $\alpha$ -Al<sub>2</sub>O<sub>3</sub> as reference material. There was also used a Diamond Perkin Elmer Thermobalance, where the experiments were achieved under identical conditions, in air, maintaining the following experimental parameters: the temperature range 20 – 500°C, heating rate of 10 °C/min and a sample mass of ~ 10 mg. FT-IR spectra of the synthesized and annealed samples were recorded on a Shimadzu-Prestige-21 spectrometer. The samples were measured as KBr pellets, in the range 400 – 4000 cm<sup>-1</sup> with a spectral resolution of 4 cm<sup>-1</sup>. XRD was used to examine the crystallinity and phase constitution of the samples prepared by the two methods. The phase evolution was investigated by Rigaku Ultima IV X-ray diffractometer using monochromatic CuK $\alpha$  radiation ( $\lambda$  = 1.54056 Å). The average crystallite size was calculated using the whole pattern profile fitting method (WPPF). The instrument influence has been subtracted using the diffraction pattern of a Si standard recorded in the same conditions. The crystalline phases were identified using JCPDS-ICDD files. The morphology and microstructure of the particles were observed by scanning electron microscopy (SEM) using a Inspect S FEI microscope (operating at 30 kV and 10-18 mm working distance).

### 3. RESULTS AND DISCUSSIONS

#### Precipitation

Results of thermal analysis measurements for the precipitate dried at 90°C are summarized in Fig.2. As one can see, there seems to be a mixture of iron hydroxides:  $\alpha$ -FeO(OH) (goethite) and  $\gamma$ -FeO(OH) (lepidocrocite). The effects on TG and DTA up to 100°C correspond to the loss of physically bound water. The effects registered up to 380°C could be attributed to the loss of structurally bound water, as well as to the topotactic and pseudomorphic dehydration of  $\alpha$ -FeO(OH) (goethite) and  $\gamma$ -FeO(OH) (lepidocrocite) [15]. In case of lepidocrocite it is known that on DTA there is an exothermic effect in the range 400 – 500°C as a result of the polymorphic transformation of  $\gamma$ -Fe<sub>2</sub>O<sub>3</sub> to  $\alpha$ -Fe<sub>2</sub>O<sub>3</sub>. The different thermal behaviour of goethite and lepidocrocite is due to the difference between their crystalline structures [16, 17].

**Figure 2:** Thermal analysis curves for the precipitate dried at 90°C



X-Ray diffraction patterns for the precipitate dried at 90°C and annealed at 200°C, 300°C and 500°C are presented in Fig.3. The samples from 90°C and 200°C are amorphous. It can be supposed that small iron oxides crystallites start forming, but the final structure is disordered. The crystallization process evolves with 300°C and it is complete at 500°C. Starting with 300°C  $\alpha$ -Fe<sub>2</sub>O<sub>3</sub> (JCPDS 01-089-2598) was the single phase identified by XRD, having a particle size of ~ 12 nm. At 500°C  $\alpha$ -Fe<sub>2</sub>O<sub>3</sub> is well crystallized with increasing particle size (~19 nm).

**Figure 3:** XRD patterns of the sample obtained by precipitation and annealed at different temperatures

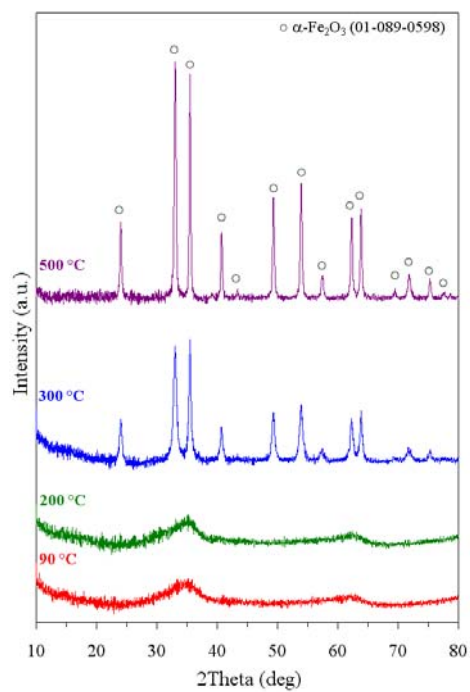
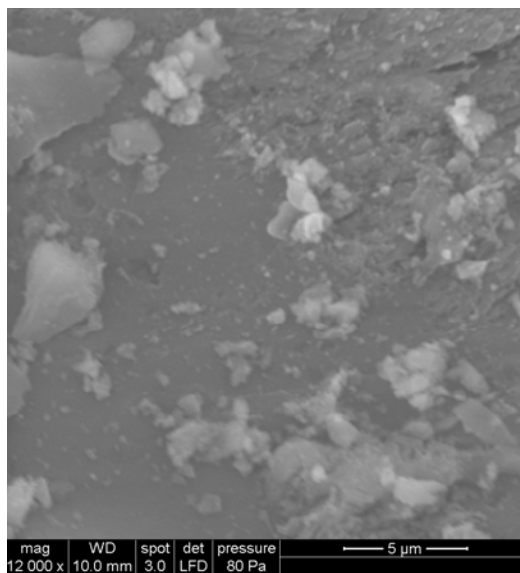


**Figure 4:** SEM image of  $\alpha$ -Fe<sub>2</sub>O<sub>3</sub> obtained at 300 °C by precipitation



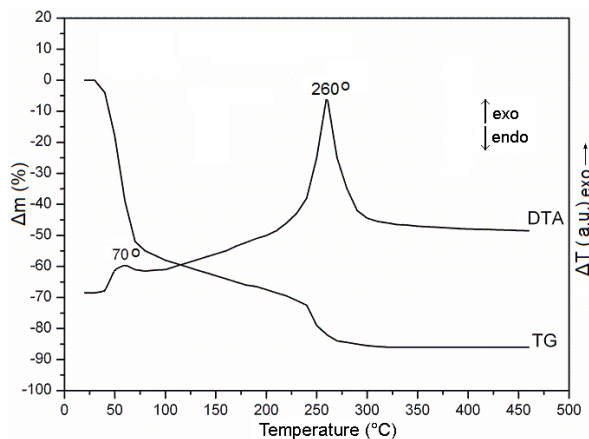
The image of the SEM micrograph (Fig.4) shows that the particles are agglomerated and have irregular shapes.

*Thermal decomposition of Fe(III) carboxylate type precursors*

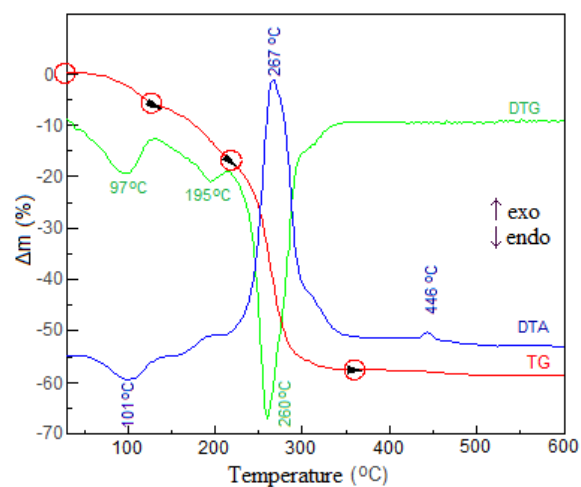
The synthesis method of the Fe(III) carboxylate type precursor consists in the solubilisation of iron nitrate in the corresponding diol amount. The resulted solution was deposited on platinum plates and heated in static air atmosphere up to 500°C on the derivatograph, in order to establish the formation mechanism of the Fe(III) carboxylate type precursor. Figure 5 presents the TG and DTA curves of the solutions  $\text{Fe}(\text{NO}_3)_3 - 1,3\text{PG}$ . The DTA curve presents two exothermic effects: a weak exothermic effect at  $\sim 70^\circ\text{C}$ , which is attributed to the redox reaction between the nitrate ion and diol with formation of the Fe(III) carboxylate type precursor. The mass loss on TG corresponding to this process is due to the water evaporation, elimination of nitrogen oxides resulted during the redox reaction and the evaporation of diol excess. The second, stronger, exothermic effect in the temperature range 250-300 °C, with a mass loss on TG, corresponds to the oxidative decomposition of the formed complex combination.

According to this study, we have established at 130°C the synthesis temperature for the oxidation products. Thus, the mixture  $\text{Fe}(\text{NO}_3)_3 - 1,3\text{PG}$  was heated, when the redox reaction between the  $\text{NO}_3^-$  ion and diol started at  $\sim 70^\circ\text{C}$  with massive gas evolving ( $\text{NO}_2$ ). The resulted product was heated at 130 °C, for 3h, until no nitrogen oxides were visible anymore, was grinded and washed with acetone in order to eliminate the unreacted diol excess.

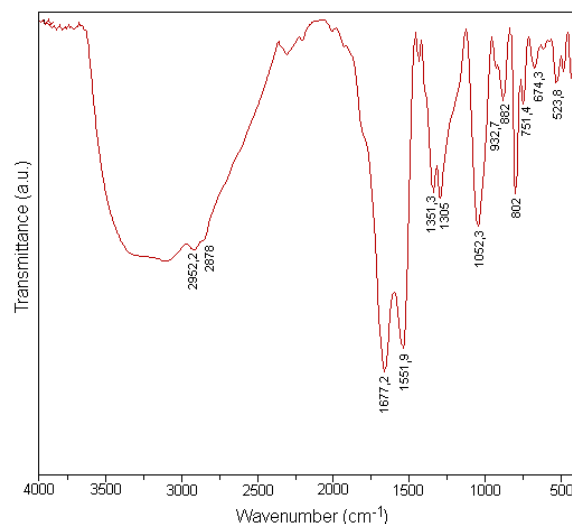
**Figure 5:** Thermal curves for the solution  $\text{Fe}(\text{NO}_3)_3-1,3\text{PG}$

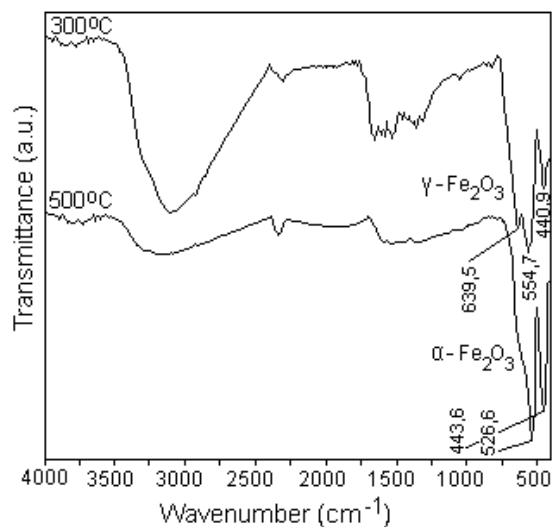


The Fe(III) carboxylate type complex combination obtained at 130°C was studied by thermal analysis and FT-IR spectrometry. The thermal behaviour from Fig. 6 indicates a mass loss up to 200°C which corresponds to the coordinated water elimination. In the temperature range 200 – 400°C takes place the oxidative decomposition with a strong exothermic effect at  $\sim 270^\circ\text{C}$  leading to  $\gamma\text{-Fe}_2\text{O}_3$ . The weak exothermic effect at  $\sim 450^\circ\text{C}$  on DTA is attributed to the polymorphic transformation of  $\gamma\text{-Fe}_2\text{O}_3$  to  $\alpha\text{-Fe}_2\text{O}_3$ . Up to 500°C, the mass loss remains constant and corresponds to the residue  $\text{Fe}_2\text{O}_3$ .

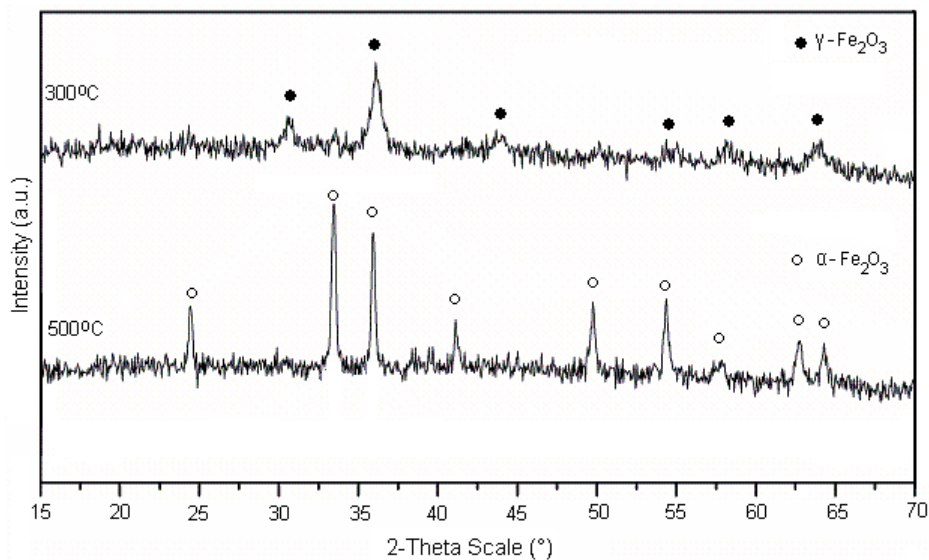
**Figure 6:** Thermal curves of the precursor obtained at 130°C

The FT-IR spectrum (Fig.7) of the precursor obtained at 130°C presents the characteristic bands for the carboxylate type complex combination  $\nu_{as}(\text{COO}^-)$  in the range 1500 – 1700  $\text{cm}^{-1}$  [18] and  $\nu_s(\text{COO}^-)$  in the range 1300 – 1400  $\text{cm}^{-1}$  [19], proving that the redox reaction was finished and the complex combination is formed. By annealing of the complex at 300°C, takes place the oxidative decomposition of the ligand ( $\text{CO}_2$  elimination) with the obtaining of a dark brown, magnetic powder ( $\gamma$ -Fe<sub>2</sub>O<sub>3</sub>). The FT-IR spectrum changes as in Fig. 8, were the bands from 639,5, 554,7 and 441  $\text{cm}^{-1}$  are present, corresponding to  $\gamma$ -Fe<sub>2</sub>O<sub>3</sub> [20]. At 500 °C, the spectrum presents the intense bands of hematite ( $\alpha$ -Fe<sub>2</sub>O<sub>3</sub>) at 526,6 and 443,6  $\text{cm}^{-1}$  [21], evidencing the transformation of  $\gamma$ -Fe<sub>2</sub>O<sub>3</sub> to  $\alpha$ -Fe<sub>2</sub>O<sub>3</sub>. The powder resulted by annealing at 500°C was red and had no magnetic properties.

**Figure 7:** FT-IR spectrum of the precursor obtained at 130°C

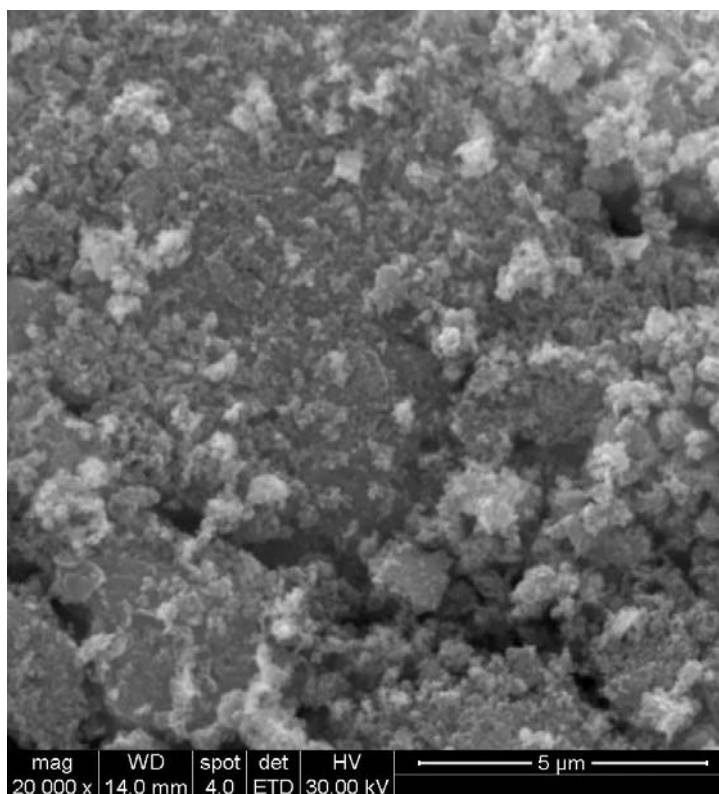
**Figure 8:** FT-IR spectra of the precursor annealed at 300°C and 500°C

The XRD patterns from Fig.9 indicate that by annealing of the Fe(III) carboxylate precursor at 300°C, the single phase is  $\gamma$ -Fe<sub>2</sub>O<sub>3</sub> while at 500°C  $\gamma$ -Fe<sub>2</sub>O<sub>3</sub> is completely transformed to  $\alpha$ -Fe<sub>2</sub>O<sub>3</sub>. The  $\alpha$ -Fe<sub>2</sub>O<sub>3</sub> nanoparticles obtained at 500°C have a mean diameter of ~ 40 nm. The SEM image (Fig.10) shows that the  $\alpha$ -Fe<sub>2</sub>O<sub>3</sub> particles are agglomerated.

**Figure 9:** XRD patterns of the samples obtained by annealing of the Fe(III) carboxylate precursor



**Figure 10:** SEM image of the sample obtained by annealing of the Fe(III) carboxylate precursor at 500°C



#### 4. CONCLUSIONS

We have synthesized  $\alpha$ -Fe<sub>2</sub>O<sub>3</sub> nanoparticles using the precipitation method and the decomposition of Fe(III) carboxylate type precursors. The studies have shown that the two synthesis methods follow different mechanisms for the obtaining of the crystalline  $\alpha$ -Fe<sub>2</sub>O<sub>3</sub>. The precipitation method has the transformation pathway iron hydroxides (goethite, lepidocrocite)  $\rightarrow$   $\alpha$ -Fe<sub>2</sub>O<sub>3</sub> (300°C) while the thermal decomposition of carboxylates method leads to the single phase  $\alpha$ -Fe<sub>2</sub>O<sub>3</sub> at 500°C, having as intermediate  $\gamma$ -Fe<sub>2</sub>O<sub>3</sub> at 300°C.

The complex combinations decomposition method is a novel method for the obtaining of  $\alpha$ -Fe<sub>2</sub>O<sub>3</sub> nanoparticles. The results are comparable to those obtained by precipitation, starting from the same reagents (iron nitrate). Among the advantages of this method may be mentioned that the synthesis procedure is faster, the yield is almost 100 % and the obtained particle size ( $\sim$  20 nm) makes  $\alpha$ -Fe<sub>2</sub>O<sub>3</sub> suitable for applications as photocatalyst in water splitting.

The advantages of the precipitation method are that  $\alpha$ -Fe<sub>2</sub>O<sub>3</sub> single phase is obtained at a lower temperature in form of nanoparticles with diameters of  $\sim$  40 nm. The method is simple and productive.

## ACKNOWLEDGEMENT

This work was partially supported by the strategic grant POSDRU/159/1.5/S/137070 (2014) of the Ministry of National Education, Romania, co-financed by the European Social Fund – Investing in People, within the Sectoral Operational Programme Human Resources Development 2007-2013.

## REFERENCES

1. Vestal, C.R.; Zhang, Z.J. Magnetic spinel ferrite nanoparticles from microemulsions. *International Journal of Nanotechnology* **2004**, *1*, 240–263.
2. Stefanescu, O.: New methods for the obtaining of  $\gamma$ -Fe<sub>2</sub>O<sub>3</sub> based nanomaterials, Doctoral thesis, Politehnica University, Timisoara, 2010.
3. Satheesh, R.; Vignesh, K.; Suganthi, A.; Rajarajan, M. Visible light responsive photocatalytic applications of transition metal (M = Cu, Ni and Co) doped  $\alpha$ -Fe<sub>2</sub>O<sub>3</sub> nanoparticles. *Journal of Environmental Chemical Engineering* **2014**, *2*, 1956–1968.
4. Teja, A.S.; Koh, P.Y. Synthesis, properties and applications of magnetic iron oxide nanoparticles. *Progress in Crystal Growth and Characterization of Materials* **2009**, *55*, 22–45.
5. Huang, M.C. The optical, structural and photoelectrochemical characteristics of porous hematite hollow spheres prepared by DC magnetron sputtering process via polystyrene spheres template. *Ceramics International* **2014**, *40*, 10537–10544.
6. Tadic, M.; Citakovic, N.; Panjan, M.; Stojanovic, Z.; Markovic, D.; Spasojevic, V. Synthesis, morphology, microstructure and magnetic properties of hematite submicron particles. *Journal of Alloys and Compounds* **2011**, *509*, 7639–7644.
7. Tadic, M.; Panjan, M.; Damnjanovic, V.; Milosevic, I. Magnetic properties of hematite ( $\alpha$ -Fe<sub>2</sub>O<sub>3</sub>) nanoparticles prepared by hydrothermal synthesis method. *Applied Surface Science* **2014**, *320*, 183–187.
8. Liang, H.; Chen, W.; Yao, Y.; Wang, Z.; Yang, Y. Hydrothermal synthesis, self-assembly and electrochemical performance of  $\alpha$ -Fe<sub>2</sub>O<sub>3</sub> microspheres for lithium ion batteries. *Ceramics International* **2014**, *40*, 10283–10290.
9. Zelenak, V.; Zelenakova, A.; Kovac, J.; Vainio, U.; Murafa, N. Influence of surface effects on magnetic behavior of hematite nanoparticles embedded in porous silica matrix. *Journal of Physical Chemistry C*, **2009**, *113*, 13045–13050.
10. Pailhe, N.; Majimel, J.; Pechev, S.; Gravereau, P.; Gaudon, M.; Demourgues, A. Investigation of nanocrystallized  $\alpha$ -Fe<sub>2</sub>O<sub>3</sub> prepared by a precipitation process. *Journal of Physical Chemistry C*, **2008**, *112*, 19217–19223.
11. Manukyan, V.; Chen, S.; Rouvimov, S.; Li, P.; Dong, S.; Liu, X.; Furdyna, J.; Orlov, A.; Bernstein, G.; Prood, W.; Roslyakov, S.; Mukasyan, A. Ultrasmall  $\alpha$ -Fe<sub>2</sub>O<sub>3</sub> superparamagnetic nanoparticles with high magnetization prepared by template-assisted combustion process. *Journal of Physical Chemistry C*, **2014**, *118*, 16264–16271.
12. Deraz, N.M.; Alarifi, A. Novel processing and magnetic properties of hematite/maghemite nano-particles. *Ceramics International*, **2012**, *38*, 4049–4055.

13. Stefanescu, O.; Stefanescu, M. New Fe(III) malonate type complex combination for development of magnetic nanosized  $\gamma$ -Fe<sub>2</sub>O<sub>3</sub>. *Journal of Organometallic Chemistry*, **2013**, 740, 50–55.
14. Stefanescu, M.; Stefanescu, O.; Stoia, M.; Lazau, C. Thermal decomposition of some metal-organic precursors. Fe<sub>2</sub>O<sub>3</sub> nanoparticles. *Journal of Thermal Analysis and Calorimetry*, **2007**, 88, 27–32.
15. Nenitescu, C.D., *General Chemistry*; Editura Didactica si Pedagogica: Bucharest, Romania, 1979.
16. Popescu, M.; Piticescu, R.; Vasile, E.; Taloi, D., Petriceanu, M.; Stoiciu, M., Badilita, V. The influence of synthesis parameters on FeO(OH)/Fe<sub>2</sub>O<sub>3</sub> formation by hydrothermal techniques. *Zeitschrift fur Naturforschung*, **2010**, 65b, 1024–1032.
17. Todor, D. *Minerals thermal analysis*; Ed. Technic: Bucharest, Romania, **1972**.
18. Nakamoto, K. *Infrared spectra of inorganic and coordination compounds*, John Wiley and Sons, New York, USA, **1970**.
19. Prasad, R.; Sulaxna; Kumar, A. Kinetics of thermal decomposition of iron (III) dicarboxylate complexes. *Journal of Thermal Analysis and Calorimetry*, **2005**, 81, 441–450.
20. Asuha, S.; Zhao, S; Wu, H.Y; Song, L.; Tegus, O. One step synthesis of maghemite nanoparticles by direct thermal decomposition of Fe-urea complex and their properties. *Journal of Alloys and Compounds*, **2009**, 472, L23–L25.
21. Yinsheng, W; Muramatsu, A.; Sugimoto, T. FT-IR analysis of well defined  $\alpha$ -Fe<sub>2</sub>O<sub>3</sub> particles. *Colloids and Surface A*, **1998**, 134, 281–297.